

## <sup>7</sup>Li and <sup>51</sup>V MAS NMR Study of the Electrochemical Behavior of Li<sub>1+x</sub>V<sub>3</sub>O<sub>8</sub>

Nicolas Dupré,<sup>†</sup> Joel Gaubicher,<sup>‡</sup> Dominique Guyomard,<sup>‡</sup> and Clare P. Grey<sup>\*,†</sup>

Chemistry Department, SUNY at Stony Brook, New York 11794-3400, and Laboratoire de Chimie des Solides, Institut des Matériaux Jean Rouxel, 2 rue de la Houssinière, B.P. 32229, 44322 Nantes cedex 3, France

Received September 11, 2003. Revised Manuscript Received April 22, 2004

<sup>7</sup>Li and <sup>51</sup>V MAS NMR spectra acquired during the electrochemical cycling of the layered battery material Li<sub>1+x</sub>V<sub>3</sub>O<sub>8</sub> have been used to follow the local structural and electronic changes that occur during the different stages of intercalation/deintercalation. Several resonances are observed using <sup>51</sup>V MAS NMR and an attempt to assign them to the different vanadium sites on the basis of the differences in the width of their sidebands manifolds is made. Both the <sup>51</sup>V and <sup>7</sup>Li NMR spectra show multiple vanadium and lithium local environments, and the spectra cannot be explained by using a simple model, based on the number of crystallographically distinct vanadium sites. Deintercalated samples with *x* close to 0 (prepared at potentials of 4.2 V vs Li) give <sup>51</sup>V spectra with very poor resolution. On lithium intercalation, the <sup>51</sup>V NMR resonances sharpen and shift to higher frequencies; three sharp resonances along with two broader resonances are clearly resolved for the samples prepared at potentials of 3.4 and 3.0 V (*x* = 0.3 and 0.5, respectively). This behavior is consistent with solid solution behavior in this potential range. Three lithium sites are observed which are assigned to the octahedral site and two tetrahedral sites between the lithium layers. The phase transition that is seen in the electrochemical data, but not with structural probes (such as X-ray diffraction), and that occurs close to 2.8 V (to form Li<sub>2</sub>V<sub>3</sub>O<sub>8</sub>), results in a decrease in the resolution of the <sup>51</sup>V resonances, and the observation of new <sup>7</sup>Li resonances at negative frequencies with much shorter relaxation times. Variable temperature experiments confirm that the shifts and short relaxation times are due to a transferred hyperfine interaction. Based on the <sup>7</sup>Li and <sup>51</sup>V spectra, the phase transition is ascribed to the formation of localized V<sup>4+</sup> and V<sup>5+</sup> ions. Further intercalation to form Li<sub>4</sub>V<sub>3</sub>O<sub>8</sub> results in the complete loss of the <sup>51</sup>V resonances and larger <sup>7</sup>Li hyperfine shifts, due to the presence of unpaired (d<sup>1</sup>) electrons.

### Introduction

The development of portable electronic devices and the need to maintain a clean environment by reducing the pollution from motorized vehicles has led to much research in the lithium-ion battery field. Over recent years, numerous studies have focused on new cathode materials for lithium cells and in particular on open-structured vanadium oxides. The characterization of the electrochemical properties of these materials, as a function of lithium ion content, represents an important step in the performance improvement process. However, these materials generally show complicated structures and it is often nontrivial to develop a detailed understanding of the electrochemical mechanisms. Li<sub>1+x</sub>V<sub>3</sub>O<sub>8</sub> is one of several oxides that have received considerable attention over the past few years as a cathode material for secondary lithium batteries.<sup>1–10</sup> Li<sub>1+x</sub>V<sub>3</sub>O<sub>8</sub> has a layered framework suitable for reversible lithium in-

tercalation processes and can allow four lithium ions per formula unit to be inserted (i.e., *x* can vary from 0 to 4). The compound forms a continuous solid solution between 4.2 and 3.0 V and shows reversible phase transitions at lower potential during cycling,<sup>11</sup> in contrast to α-V<sub>2</sub>O<sub>5</sub> where an irreversible phase transition occurs at 1.9 V. X-ray and neutron diffraction have been used to follow the distortions of the vanadium environment as a function of Li intercalation level, and to locate the Li positions between the vanadium oxide layers.<sup>12</sup> In addition to the experimental studies, ab initio density functional theory (DFT) calculations have been used to elucidate the insertion mechanisms and the origin of structural modifications, and to determine

\* To whom correspondence should be addressed.

<sup>†</sup> SUNY at Stony Brook.

<sup>‡</sup> Laboratoire de Chimie des Solides.

(1) Nassau, K.; Murphy, D. W. *J. Non-Cryst. Solids* **1981**, *44*, 297.

(2) Raistick, I. D. *Rev. Chim. Miner.* **1984**, *21*, 456.

(3) Pistoia, G.; Panero, S.; Tocci, M.; Moshtev, R. V.; Manev, V. *Solid State Ionics* **1984**, *13*, 311.

(4) Pistoia, G.; Pasquali, M.; Tocci, M.; Manev, V.; Moshtev, R. V. *J. Power Sources* **1985**, *15*, 13.

(5) Pistoia, G.; Pasquali, M.; Tocci, M.; Manev, V.; Moshtev, R. V. *J. Electrochem. Soc.* **1985**, *132*, 281.

(6) Pasquali, M.; Pistoia, G.; Manev, V.; Moshtev, R. V. *J. Electrochem. Soc.* **1986**, *133*, 2454.

(7) Bonino, F.; Ottaviani, M.; Scrosati, B.; Pistoia, G. *J. Electrochem. Soc.* **1988**, *135*, 12.

(8) Hammou, A.; Hammouche, A. *Electrochem. Acta* **1988**, *33*, 1719.

(9) de Picciotto, L. A.; Adendorff, K. T.; Liles, D. C.; Thackeray, M. M. *Solid State Ionics* **1993**, *62*, 297.

(10) Jouanneau, S.; Le Gal La Salle, A.; Verbaere, A.; Guyomard, D.; Deschamps, M.; Lascaud, S. *J. Mater. Chem.* **2003**, *13* (4), 921.

(11) Gaubicher, J.; Bourgeon, N.; Kabbour, H.; Guyomard, D. To be published.

(12) Jouanneau, S. These de Doctorat, Université de Nantes, 2001.

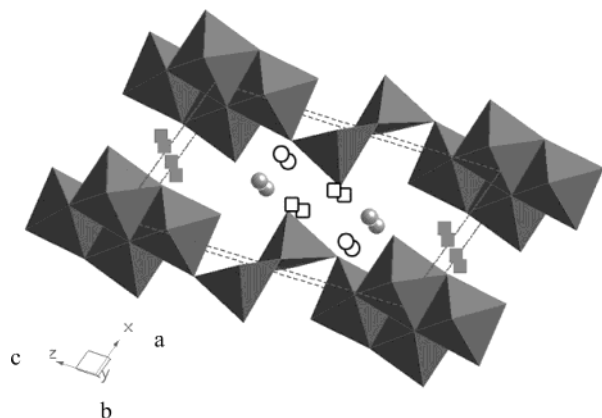


**Figure 1.** Structure of  $\text{Li}_{1+x}\text{V}_3\text{O}_8$ . The gray spheres correspond to the  $\text{Li1 } O_h$  position, and the gray squares, open squares, and open circles correspond to the  $\text{Li2}$ ,  $\text{Li5}$ , and  $\text{Li6}$  sites, respectively, which have been suggested as possible sites for Li.

which cation (Li) sites are occupied at different stages of lithiation.<sup>13,14</sup> Some contradictory results were obtained from the calculations and neutron diffraction data and many of the predictions made based on the calculations have yet to be validated experimentally.

$\text{Li}_{1+x}\text{V}_3\text{O}_8$  adopts a puckered layered structure (Figure 1) formed from edge- and corner-sharing  $\text{VO}_6$  and  $\text{VO}_5$  polyhedra. The compound crystallizes with a monoclinic lattice, with a  $P2_1/m$  space group, and contains three distinct vanadium sites: vanadium in square pyramids (V1), in distorted octahedra (V2), and in more regular octahedra (V3).<sup>15</sup> The vanadium coordination geometries become more regular on insertion of one Li ion per V atom into the interlayer space to form  $\text{V}^{4+}$  (i.e., from  $\text{LiV}_3\text{O}_8$  to  $\text{Li}_4\text{V}_3\text{O}_8$ ), the V1, V2, and V3 all adopting octahedral environments in  $\text{Li}_4\text{V}_3\text{O}_8$ . The lithium ions in  $\text{LiV}_3\text{O}_8$  are thought to sit in an octahedral ( $O_h$ ) site (Li1). Benedek et al. suggested, based on DFT calculations, that the lithium ions are inserted in several possible tetrahedral ( $T_d$ ) sites, on reduction.<sup>13</sup> Studies by Picciotto et al.<sup>9</sup> suggest that the Li2 site is the next  $T_d$  site to be occupied. By contrast, structure refinements performed by Jouanneau<sup>12</sup> of a material prepared at 350 °C with a composition between that of  $\text{Li}_{1.10}\text{V}_3\text{O}_8$  and  $\text{Li}_{1.20}\text{V}_3\text{O}_8$  found occupancies for the Li1 ( $O_h$ ), Li6 ( $T_d$ ), and Li5 ( $T_d$ ) sites of 0.924(2), 0.163(2), and 0.092(2), respectively; Li was not found on the Li2 site in this study. In another structural study of a sample ( $\text{LiV}_3\text{O}_8$ ) prepared at 580 °C, 0.82(2) Li could be refined on the Li1 ( $O_h$ ) site, whereas the remaining 0.18 Li could not be located.<sup>12</sup> All these studies were performed with X-ray diffraction and it is not always straightforward to identify all the Li sites, particularly in disordered systems.

Here, we report the use of a combination of  $^7\text{Li}$  and  $^{51}\text{V}$  MAS NMR to study the electrochemical intercalation of lithium ions within the  $\text{Li}_{1+x}\text{V}_3\text{O}_8$  matrix. The  $I = 7/2$  quadrupolar nucleus  $^{51}\text{V}$  is used to follow the changes in the vanadium local environment as a function of state of charge and  $^7\text{Li}$  is employed to study the different lithium local environments. Furthermore, both

$^7\text{Li}$  and  $^{51}\text{V}$  NMR spectroscopy are sensitive to the electronic structures of these materials and may, in principle, be used to distinguish between metallic and insulating (or semiconducting) behavior<sup>16</sup> and, thus, to provide information concerning the electronic phenomena that occur in  $\text{Li}_{1+x}\text{V}_3\text{O}_8$  electrodes during the cycling of  $\text{Li}/\text{Li}_{1+x}\text{V}_3\text{O}_8$  cells.

## Experimental Section

A material of composition  $\text{Li}_{1.17}\text{V}_3\text{O}_8$  has been synthesized according to a previously published method.<sup>3,9,15</sup>  $\text{Li}_2\text{CO}_3$  and  $\text{V}_2\text{O}_5$  were mixed in a Li/V ratio of 1.17:3 and fired at 580 °C, at 20 °C below the melting point of  $\text{Li}_{1+x}\text{V}_3\text{O}_8$  (601 °C), in a platinum crucible under air, for 24 h. This sample is labeled DS580. The firing process was interrupted after a few hours and the material was ground and then refired. A second sample was prepared by calcining a gel synthesized from  $\alpha\text{-V}_2\text{O}_5$  (0.75 mol·L<sup>-1</sup>) and  $\text{LiOH}\cdot\text{H}_2\text{O}$  (0.55 mol·L<sup>-1</sup>) mixed together at 50 °C in water for 24 h under a nitrogen atmosphere. The obtained gel was then dried by lyophilization: the gel was cooled to -40 °C and placed under a dynamic vacuum for 24 h. Thermogravimetric analysis showed that the powder contained 20% (by mass) weakly bound water after this treatment. The sample was then heated to 350 °C over 10 h to obtain an anhydrous, crystalline material, labeled SG350. The lithium content was measured by inductively coupled plasma (ICP) in emission and gave a similar composition of  $\text{Li}_{1.17}\text{V}_3\text{O}_8$  for both samples (DS580 and SG350). In principle, a material with the  $\text{Li}_{1+x}\text{V}_3\text{O}_8$  composition and  $x > 0$  implies mixed valency and the presence of  $x \text{ V}^{\text{IV}}$  ions. The composition of the starting materials was, therefore, assumed to be  $\text{Li}_{1.17}\text{V}^{\text{IV}}_{0.17}\text{V}^{\text{V}}_{2.83}\text{O}_8$ . The sample of  $\text{V}_2\text{O}_5$  was obtained from Aldrich.

An aluminum disk was coated with a slurry made by adding cyclopentanone to a mixture composed by 80% of active material, 15% of black carbon (Super P), and 5% of PVDF-HFP (Kynarflex) and dried under vacuum at ambient temperature for a few hours. A 1 M  $\text{LiPF}_6$  solution in ethylene carbonate/dimethyl carbonate (EC/DMC, (2:1) Merck) was used as the electrolyte. The cells were assembled in an argon atmosphere. Li metal was used as the negative and reference electrode. Samples were prepared electrochemically upon equilibration ( $I_{\text{min}} < 1 \text{ Li}/3000 \text{ h}$ ) at selected potentials using the potentiodynamic mode, to monitor all the major processes. The cells were then disassembled in an inert atmosphere and the cathodes were washed with anhydrous propylene carbonate to remove residual electrolyte, before packing the samples in airtight rotors for the NMR experiments.

The following NMR techniques were used to characterize the sample obtained by the solid-state synthesis route:  $^7\text{Li}$  magic angle spinning (MAS) NMR experiments were performed at operating frequencies of 77.8, 140.1, and 272.26 MHz on CMX-200, CMX-360, and Bruker DSX 700 spectrometers, corresponding to field strengths ( $B_0$ ) of 4.7, 8.4, and 16.4 T, respectively. The spectra at 4.7 T were acquired with a rotor synchronized echo sequence ( $\pi/2 - \tau - \pi - \tau - \text{acq.}$ ), where  $\tau = 1/\nu_r$  and  $\nu_r$  is the spinning frequency.  $\pi/2$  pulse widths of 2.1  $\mu\text{s}$  and pulse delays of 0.2 s were used. Spectra at 700 MHz were acquired using a single pulse sequence with a pulse delay of 0.2 s.  $^{51}\text{V}$  MAS NMR experiments were performed at operating frequencies of 52.6, 94.6, and 184.0 MHz on a CMX-200, a CMX-360, and a Bruker DSX 700 spectrometer, respectively. Spectra with spinning frequencies ( $\nu_r$ ) of 13 kHz and less were acquired with a Chemagnetics probe equipped with a 4-mm rotor, while spinning frequencies of 35 kHz were achieved by using fast MAS, 2.5-mm (700 MHz) and 2.0-mm (360 MHz) probes. All the  $^{51}\text{V}$  NMR spectra of the cathode materials and  $\text{V}_2\text{O}_5$  were acquired with a rotor synchronized ( $\pi/12 - \tau - \pi/6 - \tau - \text{acq.}$ ) echo sequence with power levels corresponding to  $\pi/2$  lengths for the liquid standard ( $\text{VOCl}_3$ ) of approximately 2–3.5

(13) Benedek, R.; Thackeray, M. M.; Yang, L. H. *Phys. Rev. B* **1999**, 60–9, 6335.

(14) Kabbour, H. *DEA Thesis (sciences des matériaux)*, Ecole Polytechnique de Nantes 2002.

(15) Wadsley, A. D. *Acta Crystallogr.* **1957**, 10, 261.

(16) Wickham, D. G. *J. Inorg. Nucl. Chem.* **1965**, 27, 1939.

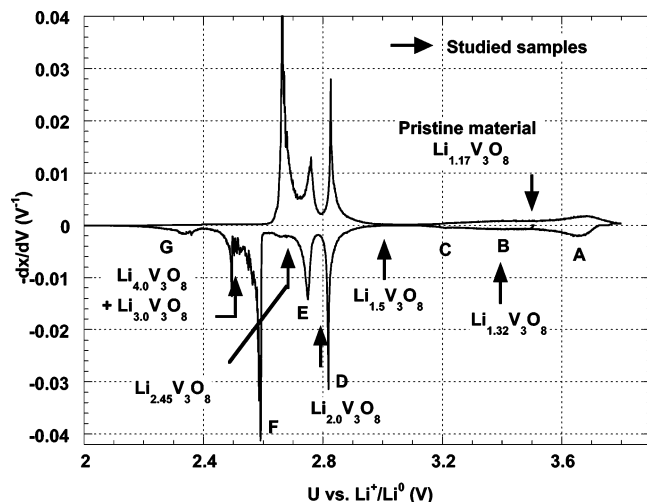


**Figure 2.** Cyclic voltammogram obtained in potentiodynamic mode for the first cycle (the two first reductions and the first oxidation), between 3.8 and 2.0 V for  $\text{Li}_{1+x}\text{V}_3\text{O}_8$  with a rate of 1.25 mV/h and a cutoff current corresponding to 1 Li/100 h. The different processes seen on discharge are labeled A–F.

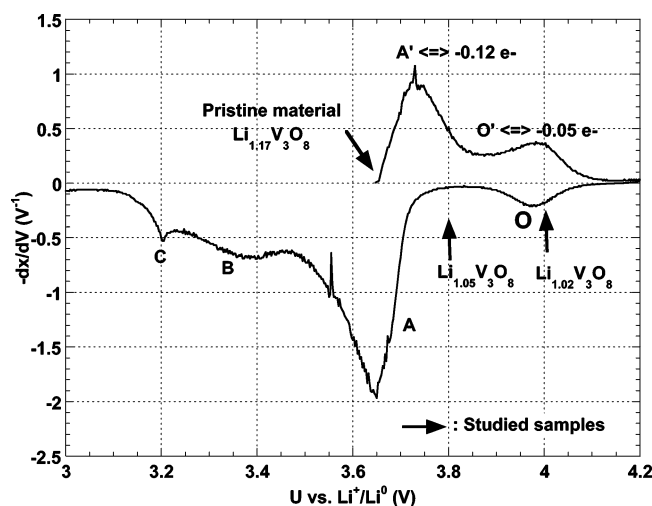


**Figure 3.** Cyclic voltammogram obtained in potentiodynamic mode on the first oxidation and reduction, between 4.2 and 3.0 V, for  $\text{Li}_{1+x}\text{V}_3\text{O}_8$  with a rate of 1.25 mV/h and a cutoff current corresponding to 1 Li/100 h. The different processes seen are labeled A' and O' on charge and O, A–C on discharge.

$\mu\text{s}$ , the shorter pulse lengths being achieved on the fast MAS probes. Spectra were obtained at different spinning speeds (9 and 13 kHz) on the CMX-360 spectrometer, to determine the frequency of the isotropic resonances, except where the signals were so broad that individual spinning sidebands could not be resolved. The  $^7\text{Li}$  and  $^{51}\text{V}$  spectra were referenced to 1 M LiCl solution and  $\text{VOCl}_3$ , respectively, as external references, both at 0 ppm.

Spin–lattice relaxation times ( $T_1$ ) were measured using an inversion–recovery sequence ( $\pi - \tau_D - \pi/2 - \text{acq.}$ ), where  $\tau_D$  is a delay under our control.

## Results and Discussion

**Electrochemistry.** The first electrochemical cycle of  $\text{Li}/\text{Li}_{1+x}\text{V}_3\text{O}_8$  (DS580), starting with a reduction, is presented in Figure 2. Figure 3 shows the electrochemical cycle of a second cell obtained by first charging the cell to 4.2 V (vs Li) followed by a subsequent cycle between 3.8 and 2.0 V. The open circuit voltage (OCV) of the starting material is approximately 3.65 V, but

**Table 1. Potential of Equilibrated Cells Used To Prepare the Samples for NMR Spectroscopy and the Compositions of the Resulting Cathode Materials**

potential (V)	4.02	3.80	3.65	3.40	3.00	2.80	2.70	2.50
composition	0.02	0.05	0.17	0.32	0.5	1.0	1.45	2.30 <sup>a</sup>
$x$ in $\text{Li}_{1+x}\text{V}_3\text{O}_8$								

<sup>a</sup> A 70:30 mixture of  $\text{Li}_3\text{V}_3\text{O}_8$  and  $\text{Li}_4\text{V}_3\text{O}_8$ .

varies slightly between samples and different cells. 0.17  $\text{Li}^+$  can be extracted from the cathode material on charging the cell, consistent with the stoichiometry of the material obtained by ICP. A number of electrochemical processes are observed both on charging and then subsequent discharging, consistent with a recent evaluation of the electrochemical behavior.<sup>11,17</sup> In contrast to earlier electrochemical studies, four separate processes (O, A, B, and C) were identified in the solid solution region ( $\text{Li}_{1.0}\text{V}_3\text{O}_8 - \text{Li}_{1.5}\text{V}_3\text{O}_8$ ).<sup>12,14</sup> More than one phase transition occurs between the compositions  $\text{Li}_{1.5}\text{V}_3\text{O}_8$  and  $\text{Li}_5\text{V}_3\text{O}_8$  (D to G). One of them (labeled D), however, could not be confirmed in the XRD or TEM experiments and as a consequence does not seem to be associated with a structural transformation.

Seven samples were prepared from the original DS580 sample to investigate the various electrochemical processes. The purity of each sample was checked by XRD. Two deintercalated samples were equilibrated at 4.20 V ( $\text{Li}_{1.02}\text{V}_3\text{O}_8$ ) and at 3.80 V ( $\text{Li}_{1.05}\text{V}_3\text{O}_8$ ), after an initial oxidation to 4.20 V (Figure 3). The sample  $\text{Li}_{1.0}\text{V}_3\text{O}_8$  (4.20 V) could not be obtained by electrochemical oxidation because it was not stable to electrolyte oxidation. Attempts to stabilize the sample at 4.20 V resulted systematically in an open circuit voltage (OCV) drop to 4.02 V, before the battery could be unpacked. This potential corresponds roughly to the center of the high potential peak (O). A further 0.02  $e^-$  could be extracted following subsequent recharging of the same cell up to 4.20 V. The composition of the 4.02 V sample was, therefore, assumed to be  $\text{Li}_{1.02}\text{V}_3\text{O}_8$ . A set of five further intercalated samples were prepared by discharging fresh cells and equilibrating at 3.4 V ( $\text{Li}_{1.32}\text{V}_3\text{O}_8$ ), 3.0 V ( $\text{Li}_{1.5}\text{V}_3\text{O}_8$ ), 2.8 V ( $\text{Li}_2\text{V}_3\text{O}_8$ ), and 2.7 V ( $\text{Li}_{2.45}\text{V}_3\text{O}_8$ ) (Figure 2). The final cell was stopped at 2.5 V, before the completion of the intercalation process that starts at 2.61 V, so that both the phases  $\text{Li}_3\text{V}_3\text{O}_8$  and  $\text{Li}_4\text{V}_3\text{O}_8$  are present in the samples (see Figure 2). The compositions and potentials of the different samples are summarized in Table 1.

**$^7\text{Li}$  MAS NMR.** The Li MAS NMR spectra were acquired from the pristine DS580 sample and the seven charged/discharged samples (Figure 4). Only one resonance was seen at low fields (4.7 and 8.4 T, spectra not shown), even when high spinning frequencies were used, and the use of a 16.4 T field strength (700 MHz) was needed to resolve the different resonances for the samples equilibrated at potentials above 2.8 V. Three resonances are seen in the spectrum of the pristine material, at  $-7.0$ ,  $-5.0$ , and  $-2.9$  ppm. Deconvolution of the spectrum gives approximate intensities of these resonances of 90, 6, and 4%, respectively. These values are close to concentrations of the different sites obtained from the structure refinements of SG350<sup>13</sup>: 80% (Li1 site), 13% (Li6 site), and 7% (Li5 site), considering the



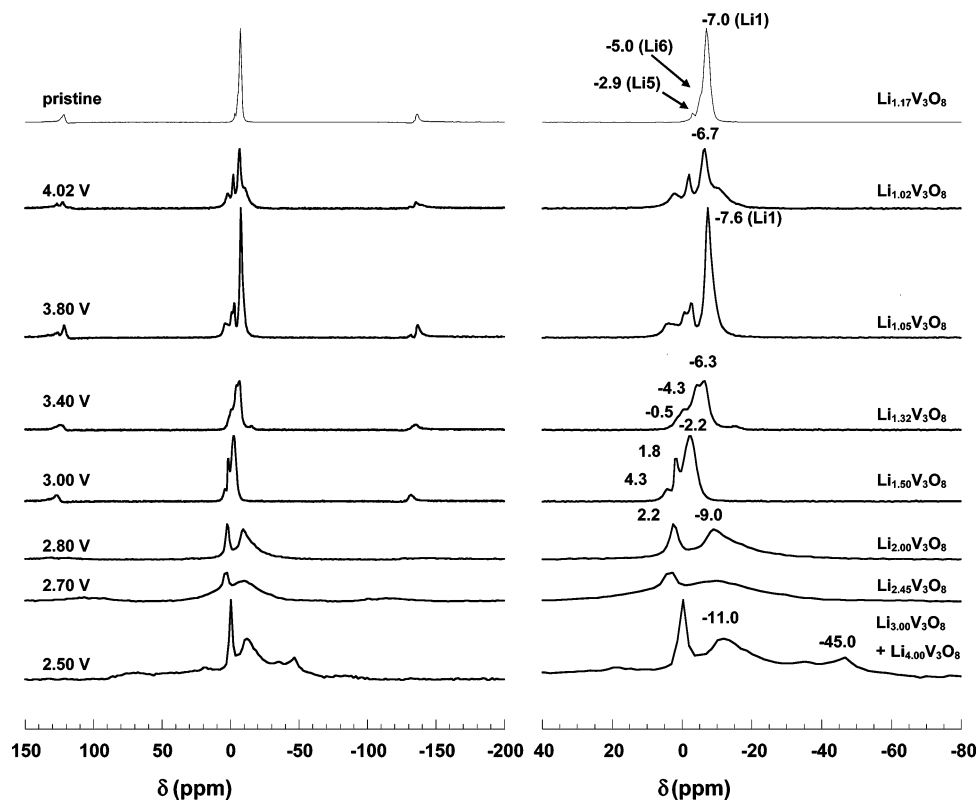


**Figure 4.**  $^7\text{Li}$  MAS NMR spectra of  $\text{Li}_{1+x}\text{V}_3\text{O}_8$  obtained at different stages of the intercalation process, acquired at  $B_0 = 16.4$  T and at a spinning speed of  $\nu_r = 35$  kHz. The 2.7 V spectrum has been acquired at 16.4 T and at a spinning speed of  $\nu_r = 30$  kHz. The 2.5 V spectrum has been acquired at 4.7 T and at a spinning speed of  $\nu_r = 35$  kHz. A very similar spectrum was obtained at 16.4 T but with a lower resolution, and then the 4.7 T spectrum has been plotted for the sake of clarity. All the spectra (except the 2.5 V one) have been plotted in an absolute intensity mode. An enlargement of the spectra, showing the isotropic resonances, is plotted on the right-hand side.

precision that can be achieved with both experimental methods. On oxidation to 4.02 V, a number of new resonances become visible. Reduction of the pristine sample (OCV  $\sim 3.65$  V) down to 3 V results in a gradual slight shift of the Li resonances to higher frequency and a change in intensities of the different resonances.

Since the peak at  $-6.7$  ppm in the 4.02 V spectrum is the most intense, it may be assigned to the Li(1) site. However, there are a large number (at least four) of Li local environments, even at the highest potential investigated, that is, compositions around  $\text{Li}_1\text{V}_3\text{O}_8$ , indicating that the Li ions do not solely occupy the Li(1) site as suggested in earlier XRD studies.<sup>12</sup> The four different electrochemical processes in the 4.2–3.0 V region indicate that intercalation/deintercalation occurs from different lithium sites and/or that lithium rearrangements occur within the structure during cycling. The changes in the chemical shifts and intensities of the resonances (in particular the decrease of the intense resonance assigned to Li1) on oxidizing the pristine material to the 4.02 V sample indicate that both Li extraction and rearrangement of the Li ions between the layers occurs on oxidation. On reduction to 3.8 V ( $\text{Li}_{1.05}\text{V}_3\text{O}_8$ ) on the subsequent discharge, the intensity of the resonance assigned to the Li1 site ( $\delta = -7.6$  ppm) increases again and dominates the spectrum of this material. This suggests that the “O” process involves the filling of the Li(1) site, by a combination of Li addition of  $\text{Li}^+$  and  $\text{Li}^{+}$ -ion rearrangement.

Three major resonances are again observed in the spectra of samples stabilized at a potential below 3.80

V (i.e., the 3.40 and 3.00 V samples). For the 3.40 V sample, three resonances are seen at  $-6.3$ ,  $-4.3$ , and  $-0.5$  ppm, the resonances shifting to, respectively  $-2.2$ ,  $1.8$ , and  $4.3$  ppm at 3.0 V. Since no satisfactory deconvolution of the resonances was obtained due to a severe overlap of the resonances, no clear assignment of the different lithium sites in the host material to the observed resonances can be made and only the general evolution of the system could be followed. The pristine material (OCV = 3.65 V) and the sample equilibrated at 3.4 V show a small difference in lithium intercalation level ( $\Delta x = 0.13 \text{ Li}^+$ ). Since the Li content and shape of the spectra of these materials are close, it seems reasonable to use the assignments of the pristine material to assign the 3.40 V NMR resonances. Thus, the resonances at  $-6.3$ ,  $-4.3$ , and  $-0.5$  ppm are assigned to the Li1, Li6, and Li5 sites, respectively. When the spectrum of the 3.4 V material is compared with that of the pristine material, all the peaks undergo only a very small shift ( $\Delta\delta = 0.7$  ppm) except the peak attributed to the Li5 site ( $\Delta\delta = 2.5$  ppm), suggesting that this site is more sensitive to the reduction of the vanadium layers. This site is associated with the largest increase in intensity, while the Li1 site drops in intensity, suggesting that the B process involves the population of the Li5 site and the rearrangement of the Li ions between the layers. DFT results<sup>14</sup> suggest that V3 is preferentially reduced above 2.6 V. Thus, by implication, Li6, which is closer to the V3 site, should be more sensitive to reduction. However, the NMR results indicate a complicated process involving both

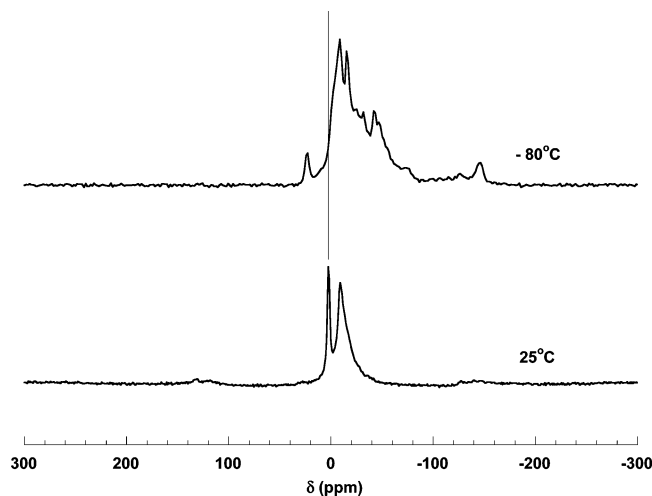


**Figure 5.**  $^7\text{Li}$  MAS NMR spectra of  $\text{Li}_{2.0}\text{V}_3\text{O}_8$  (2.8 V) obtained at ambient temperature and  $-80\text{ }^\circ\text{C}$ , acquired respectively at  $B_0 = 16.4\text{ T}$ ,  $\nu_r = 35\text{ kHz}$  and  $B_0 = 4.7\text{ T}$ ,  $\nu_r = 15\text{ kHz}$ .

lithium insertion and rearrangement in this range, and it is not straightforward from these results to determine whether a specific vanadium site is reduced.

On lowering the potential from 3.4 to 3.0 V, larger shifts ( $\Delta\delta$  between 4.10 and 6 ppm) are observed for all the resonances. Now, the largest shift is seen for the resonance attributed to the Li6 site, at 4.3 ppm in the 3.0 V spectrum ( $\Delta\delta = 6.1\text{ ppm}$ ), and this site now seems to be more sensitive to reduction. Relaxation times ( $T_1$ ) measurements for samples in the 4.2–3.0 V range gave values between 220 and 420 ms for all the  $^7\text{Li}$  NMR resonances.

We note that the assignments given above are not definitive. For example, it would also be possible to assign both the  $-4.3$  and  $-6.3\text{ ppm}$  resonances to two Li1 sites with different arrangements of nearby Li ions. Independent of the assignments, what is clear, however, is that the large number of peaks in the cyclic voltammogram arise from the filling of different sites and the rearrangements of the Li ions among the different sites, presumably to minimize  $\text{Li}^+ - \text{Li}^+$  interactions. The results suggest small differences in the energies of the different configurations for Li in the layers. It is clear that a simple model where one or two lithium sites are filled progressively cannot describe the behavior of the compound during the intercalation at high potentials.

Very different behavior is seen for the samples discharged to below 3 V. At 2.8 V ( $\text{Li}_2\text{V}_3\text{O}_8$ ), a new, broad resonance appears at between  $-8$  and  $-20\text{ ppm}$ , a second even lower, broad frequency resonance ( $-45\text{ ppm}$ ) being observed for the 2.5 V sample which contains both the  $\text{Li}_3\text{V}_3\text{O}_8$  and  $\text{Li}_4\text{V}_3\text{O}_8$  phases. The latter phase, containing all  $\text{V}^{\text{IV}}$  ions and an additional lithium ion,<sup>18</sup> probably gives rise to the resonance at  $-45\text{ ppm}$ . On lowering the temperature to  $-80\text{ }^\circ\text{C}$ , the resonances observed for the 2.8 V sample (Figure 5) shift noticeably to lower frequency and at least eight new resonances are resolved. Much shorter spin–lattice ( $T_1$ ) relaxation times were obtained at room temperature for the resonances observed at negative frequencies (5 ms for the  $-8$  to  $-20\text{ ppm}$  resonance, in contrast to 140 ms

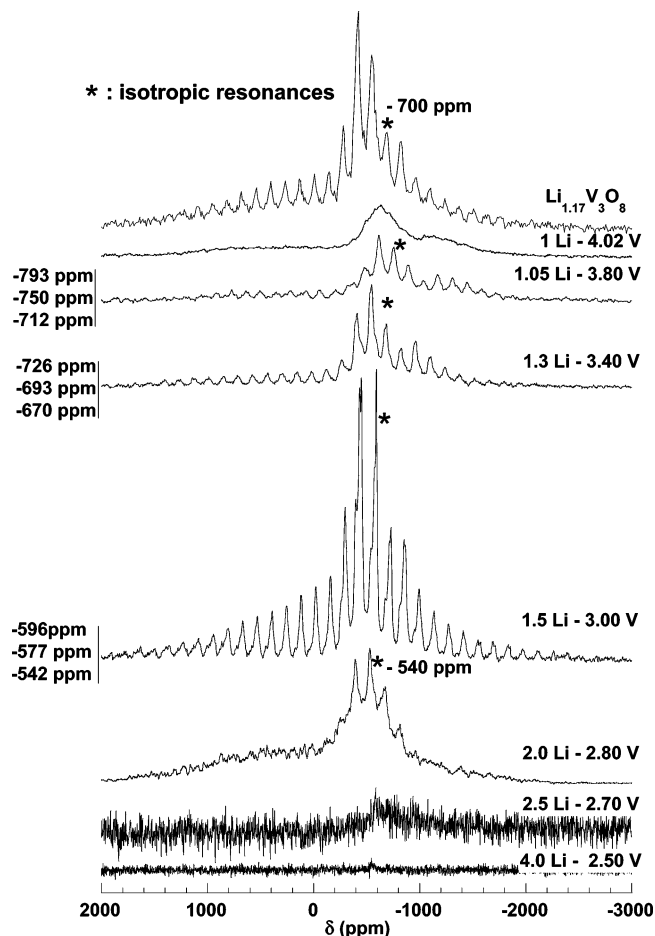


**Figure 6.**  $^{51}\text{V}$  MAS NMR spectra of  $\text{Li}_{1+x}\text{V}_3\text{O}_8$  obtained at different stages of the intercalation process, acquired at  $B_0 = 8.4\text{ T}$ ,  $\nu_r = 13\text{ kHz}$ . The spectra are plotted in a quantitative mode, where the intensity has been scaled to take into account differences in sample acquisition numbers and sample weights. The isotropic resonances are marked with asterisks; all the other peaks are spinning sidebands. The shifts of the isotropic resonances are marked either next to the peaks or next to the spectra for the sake of clarity.

for the resonance at 2.2 ppm). These short relaxation times are consistent with the presence of unpaired electrons in the Li local coordination sphere. A very long recovery time ( $T_1 = 2.7\text{ s}$ ) was measured for the most intense peak in the 2.5 V sample, seen at 0 ppm. Thus, this resonance does not appear to be due to a site in the cathode material and is assigned to the  $\text{Li}^+$  ions in diamagnetic local environments, possibly on the surface of the particles, due to the unremoved  $\text{Li}^+$  ions in the electrolyte and/or SEI layer formation.

**$^{51}\text{V}$  MAS NMR.** The  $^{51}\text{V}$  spectrum of the pristine material  $\text{Li}_{1.17}\text{V}_3\text{O}_8$ , obtained at a spinning speed of 13 kHz, consists of a broad isotropic resonance at approximately  $-700\text{ ppm}$  and a series of sidebands that span over more than 3000 ppm (Figure 6). The outer sidebands are due to the  $^{51}\text{V}$  satellite transitions of the  $I = 7/2$  nucleus. The resolution was not good enough to distinguish resonances due to different vanadium environments. At high potential (4.02 V), a much broader signal is observed with a center of mass at approximately  $-800\text{ ppm}$ . As lithium ions are intercalated within the structure and the  $\text{V}^{5+}$  is partially reduced to  $\text{V}^{4+}$ , the isotropic resonances and their sidebands progressively sharpen and are resolved more

(18) Benedek, R.; Thackeray, M. M.; Yang, L. H. *Phys. Rev. B* **1997**, 56–17, 10707.

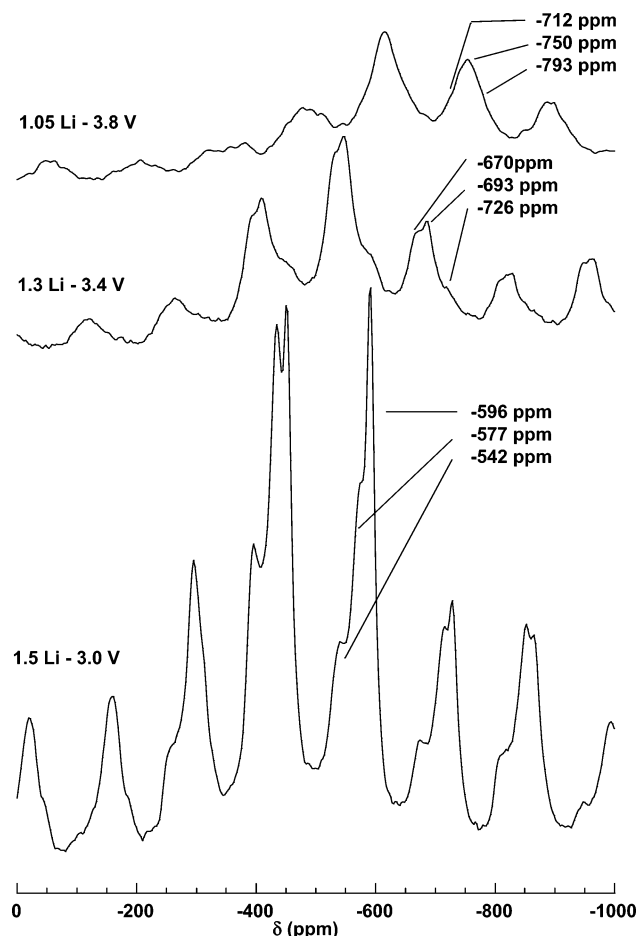


**Figure 7.** Blowup of the  $^{51}\text{V}$  MAS NMR spectra of  $\text{Li}_{1+x}\text{V}_3\text{O}_8$  obtained at 3.8, 3.4, and 3.0 V of the intercalation process, acquired at  $B_0 = 8.4$  T and  $\nu_r = 13$  kHz.

clearly. The sample stabilized at 3.8 V shows at least three resonances, the most apparent, after the deconvolution of the isotropic resonances and their spinning sidebands, being seen at  $-790 \pm 20$ ,  $-750 \pm 20$ , and  $-710 \pm 20$  ppm. A continuous shift toward higher frequencies is observed, as lithium is intercalated into the host material (Figures 6 and 7), the three resonances found at  $-726$ ,  $-693$ , and  $-670$  ppm for the 3.4 V sample shifting to  $-542$ ,  $-596$ , and  $-577$  ppm for the 3.0 V sample, respectively. The spectra of the 3.4 and 3.0 V samples, acquired at a higher spinning speed (35 kHz), clearly showed additional resonances at  $-610$  and  $-800$  ppm and  $-625$  and  $-690$  ppm, respectively (Figure 8). These resonances must be masked by the three main resonances in the spectra acquired at lower spinning speeds. These new resonances cannot be attributed to unreacted material since the resonances shift with lithium intercalation level. No additional resonances were observed in the fast spinning spectra of the other samples presumably due to the poor resolution of these spectra. The continuous shift of all the resonances from 3.8 to 3.0 V is consistent with the solid solution intercalation behavior in this region and is in agreement with conclusions made on the basis of the  $^7\text{Li}$  MAS NMR data. Reduction to 2.8 V results in a dramatic change in the spectrum, the resonances broadening considerably so that the different features are barely observable. Further reduction to 2.7 and 2.5 V leads to a complete loss of the  $^{51}\text{V}$  NMR signal.

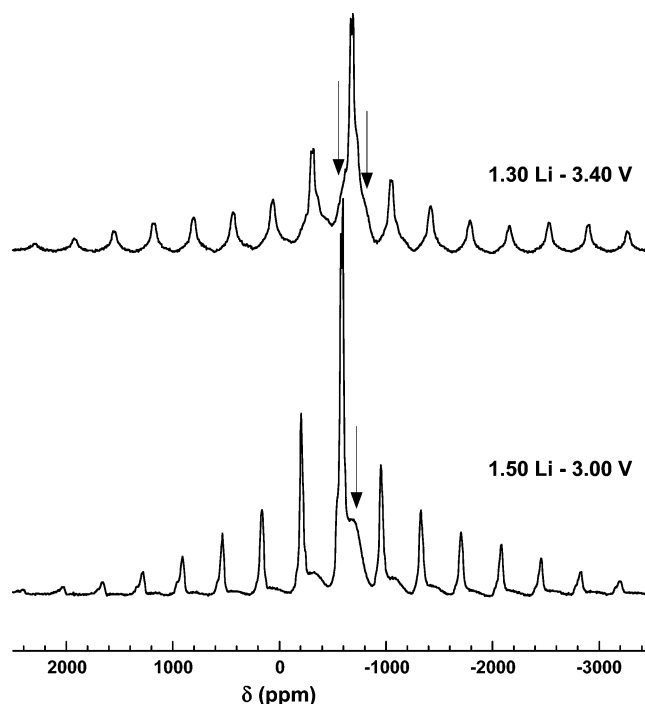


**Figure 8.**  $^{51}\text{V}$  MAS NMR spectra of  $\text{Li}_{1+x}\text{V}_3\text{O}_8$  obtained at 3.4 and 3.0 V, acquired at  $B_0 = 8.4$  T,  $\nu_r = 35$  kHz. The arrows mark the additional resonances observed at higher spinning frequencies.

The spectra of the two different starting materials, obtained by varying the synthesis route, show noticeable differences:  $\text{Li}_{1.17}\text{V}_3\text{O}_8$  (SG350) contains smaller crystallites and gives a better resolved  $^{51}\text{V}$  NMR spectrum than the well-crystallized  $\text{Li}_{1.17}\text{V}_3\text{O}_8$  (DS580) prepared by the solid-state route. Chemical titration and electrochemical deintercalation experiments give the same  $\text{V}^{4+}$  content for both materials, suggesting that the  $\text{V}^{4+}$  concentration is not at the origin of the different behaviors of the two materials. In addition,  $^7\text{Li}$  MAS NMR spectra for these two samples, although very similar, show slight differences: the spectrum of SG350 shows broader resonances that can be assigned to a distribution of shifts, supporting the presence of defects in SG350. Chemical shifts are observed at  $-7$ ,  $-5$ , and  $-3$  ppm for DS580 and  $-9$ ,  $-5$ , and  $-1.5$  ppm for SG350, corresponding to slightly different local environments. The ratios of the area of the three signals are, however, the same for both samples and thus could be assigned to the same crystallographic sites (i.e., Li(1), Li(6), and Li(5)).

To attempt to assign the vanadium signals to different local environments, we analyzed the sidebands of the  $^{51}\text{V}$  resonances obtained for the higher voltage samples in greater detail. Three sites were observed in the 3.8, 3.4, and 3.0 V samples, at 360 MHz and a spinning speed of 15 kHz. From previous  $^{51}\text{V}$  studies,<sup>19</sup> it is known that  $\text{V}^{5+}$  in a distorted octahedral environment exhibits both a large quadrupolar coupling constant and chemical shift anisotropy, resulting in large sideband manifolds resonances.<sup>19,20</sup> Large sideband manifolds are similarly observed for distorted pentacoordinated va-

(19) Skibsted, J.; Jacobsen C. J. H.; Jakobsen, H. J. *Inorg. Chem.* **1998**, 37, 3083.

(20) Shubin, A. A.; Lapina, O. B.; Courcot, D. *Catal. Today* **2000**, 56, 379.

nadium sites as in  $\text{V}_2\text{O}_5$ <sup>19–21</sup> or vanadyl phosphates<sup>19,22</sup> (quadrupole coupling constant,  $C_Q = 825$  kHz for  $\alpha\text{-VOPO}_4$  and  $C_Q = 1990$  kHz for  $\beta\text{-VOPO}_4$ ). For the 3.8 V sample, the different resonances are strongly overlapping, although it is still possible to resolve three sets of spinning sidebands partially. Since one resonance (−793 ppm) is associated with larger sideband manifolds, it is likely due to a very distorted environment. The two other resonances (−750 and −712 ppm) show smaller sideband manifolds and are assigned to less distorted environments. The three resonances at −726, −693, and −670 ppm (Figure 6 and Figure 7) for the 3.4 V sample appear to be related to the resonances at −793, −750, and −712 ppm, respectively, of the 3.8 V sample, based on the intensities of isotropic resonances and the shape of the sideband manifolds. The change in the  $^{51}\text{V}$  shift is clearly related to the change in intercalation level. The weakest resonance at −793 ppm in the 3.8 V sample spectrum undergoes a larger shift on reduction than the other two resonances, suggesting that this vanadium environment is more affected by the lithium intercalation in this potential range.

Simulations of the full 3.4 and 3.0 V MAS spectra (including both the central and satellite transitions) were performed by using the Simpson program.<sup>23</sup> An accurate determination of these parameters was not possible due to the strong overlap of the different resonances and the following results are only provided so as to illustrate the differences in the distortions of the different sites. The relative orientation of the electric field gradient and chemical shift tensors could not be determined with any precision since the changes in the quadrupolar constants (QCC) and chemical shielding anisotropy (CSA) observed when varying the relative orientations of the tensors were within the errors of these simulations. The two sharpest resonances at −596 and −573 ppm for the 3.0 V sample are associated with relatively small QCCs, respectively, of 0.7 and 0.9 MHz, but with large values of the asymmetry parameter (respectively,  $\eta_Q = 0.8$  and  $\eta_Q = 0.9$ ) and small CSAs ( $\eta_{\text{CSA}} = 0.1\text{--}0.3$ , a chemical shift anisotropy  $\sigma_{\text{ani}} = \sigma_{33} - \sigma_{11} =$  approximately 600 ppm). The QCC increases slightly to 1 MHz at 3.4 V, the other parameters remaining unchanged. The resonance at −596 ppm, whose shift is also the most sensitive to lithium intercalation level, is tentatively assigned to the most symmetric vanadium environment (i.e., the V3 environment). The −573 ppm resonance is then assigned to the V2 site. The third sharper resonance at −540 ppm with the largest QCC (1.5 MHz) has similar values for the CSA as the other sites. This resonance is tentatively assigned to the V1 site. No significant change in the parameters is seen for the third resonance between the spectra obtained at 3.0 and 3.4 V.

The study performed at a high spinning speed (35 kHz) clearly showed additional resonances for the 3.4 (−610 and −800 ppm) and 3.0 V (−625 and −690 ppm) samples (Figure 8). These sites are associated with even

larger QCCs of 2 MHz ( $\eta_Q = 0.9$  and  $\eta_Q = 0.9$ , respectively) and values of  $\sigma_{\text{ani}}$  of the order of 800 ppm. The observation of these resonances indicates that a model in which the three different vanadium crystallographic sites are assigned to the sharp  $^{51}\text{V}$  resonances is too simple to explain the spectra of these materials. This result is consistent with the filling of a variety of different lithium sites as found by  $^7\text{Li}$  MAS NMR, differences in the occupancies of the Li sites in the Li layers, resulting in different vanadium local environments and different  $^{51}\text{V}$  resonances. Different vanadium resonances may result depending on whether the vanadium sites have lithium neighbors on a Li(5) site, on a Li(6) site, on both sites, on a Li1 site, or no lithium neighbors. We tentatively assign the two sets of resonances to vanadium nearby additional Li, and vanadium more distant from Li.

**NMR Shift Mechanisms: Implications for Electronic Structure.** In addition to the chemical shift, the NMR spectra of  $\text{V}^{4+}$ -containing materials may be affected by either hyperfine or Knight shifts. Knight shifts are seen in metals and the shift is a measure of the density of states at the Fermi level  $N(E_F)$  of the nucleus under investigation ( $^7\text{Li}$  or  $^{51}\text{V}$ ). Fermi-contact (hyperfine) interactions are caused by unpaired electrons, the size of the shift being a measure of the unpaired electron spin density transferred from the paramagnet (e.g.,  $\text{V}^{4+}$ ;  $d^1$ ) to the s orbitals of the Li ions and are responsible for the large shifts seen for many  $\text{V}^{4+}$  compounds. For example, large hyperfine shifts of around +100 ppm were observed in the Li NMR of a variety of  $\text{V}^{4+}$  compounds such as  $\alpha\text{-LiVOPO}_4$  or  $\text{LiV}_2(\text{PO}_4)_3$ .<sup>22,24</sup> Smaller negative shifts have been observed for Li-intercalated  $\text{V}_2\text{O}_5$  ( $-2.1 < \delta < -31.4$  ppm), xerogels (−25 ppm), and aerogels (−22 ppm),<sup>25–27</sup> which all contain edge- and corner-sharing  $\text{VO}_5/\text{VO}_6$  layers and chains. The hyperfine interaction is proportional to the magnetic susceptibility of the paramagnets, and thus hyperfine shifts can be extremely temperature-dependent.

The behavior of samples discharged to below 3 V is consistent with the presence of localized unpaired electrons in the Li local coordination sphere. Short  $^7\text{Li}$  T<sub>1</sub>s, temperature-dependent behavior, and large negative shifts are seen, all consistent with the hyperfine (Fermi-contact) shifts observed in layered  $\text{V}^{4+}$ -containing compounds such as  $\text{V}_2\text{O}_5$ . A number of different local environments are observed at low temperatures for the 2.8 V sample; these local environments are not resolved at room temperature, indicating some mobility of the Li ions, or possibly some hopping of the electrons at room temperature in this mixed  $\text{V}^{4+}/\text{V}^{5+}$  phase. The large number of local environments seen at low temperatures is indicative of the structural disorder of the material.

The  $^{51}\text{V}$  NMR spectra of the <3 V samples are also consistent with localized  $d^1$  electrons: previous studies

(21) Lapina, O. B.; Khabibulin, D. F.; Shubin, A. A.; Bondareva, V. M. *J. Mol. Catal. A* **2000**, *162*, 381.

(22) Dupre, N.; Gaubicher, J.; Siegel, R.; Brunelli, M.; Hirschinger, J.; Querton, M. Submitted.

(23) Baks, M.; Rasmussen, J. T.; Nielsen, N. C. *J. Magn. Res.* **2000**, *147* (2), 296.

(24) Gaubicher, J.; Wurm, C.; Goward, G.; Masquelier, C.; Nazar, L. *Chem. Mater.* **2000**, *12*, 3240.

(25) Savariault, J. M.; Deramond, E.; Galy, J.; Mongrelet, T.; Hirschinger, J. *Mol. Cryst. Liq. Cryst.* **1994**, *244*, 367.

(26) Holland, G. P.; Buttry, D. A.; Yarger, J. L. *Chem. Mater.* **2002**, *14*, 3875.

(27) Stallworth, P. E.; Johnson, F. S.; Greenbaum, S. G.; Passerini, S.; Flowers, J.; Smyrl, W. *J. Appl. Phys.* **2002**, *92*–7, 3839.



showed that  $^{51}\text{V}$  NMR spectra of  $\text{V}^{\text{IV}}$  compounds, with localized  $d^1$   $\text{V}^{4+}$  ions, are typically "invisible" by NMR, when standard MAS NMR methods are used. The dramatic loss of  $^{51}\text{V}$  signal and broadening of the peaks in the spectrum of the 2.8 V sample is consistent with the presence of  $\text{V}^{4+}$  ions, which will broaden the signals from the vanadium sites. The total absence of signal after stabilization at 2.5 V indicates that essentially all the vanadium ions are reduced to  $\text{V}^{4+}$  consistent with the stoichiometry of the sample.

Three volts represents the limit of the solid solution range and a phase transition is seen (in the cyclic voltamogram) on lowering the potential to 2.8 V (D  $\rightarrow$  E). There is a distinct difference between the  $^7\text{Li}$  and  $^{51}\text{V}$  NMR spectra observed below 3 V and at 3 V and above and the NMR results are consistent with a phase transition that is electronic in nature. No structural phase transition is seen with structural probes such as XRD and TEM,<sup>28</sup> again suggesting that this is an electronic phase transition.

Both the small  $^7\text{Li}$  shifts and long  $T_1$  times (220–420 ms) for the 3.0–4.0 V samples do not appear to be consistent with the presence of large Li–O– $\text{V}^{4+}$  hyperfine interactions. For example, the 3.0 V sample ( $\text{Li}_{1.5}\text{V}_3\text{O}_8$ ) has an average vanadium oxidation state of +4.83, yet shifts of no more than 7 ppm are seen from the shift position of the diamagnetic standard, LiCl. Furthermore, on lowering the temperature to  $-80^\circ\text{C}$ , no shifts in the resonances of the pristine material are seen (data not shown). There are two possible explanations for these observations. First, the small shifts could arise from Knight shifts. Metallic samples such as Li metal and lithium intercalated in carbon electrodes show isotropic resonances at higher frequencies (250 ppm and 10–72 ppm, respectively<sup>29,30</sup>). The smaller shifts seen in this system can then be ascribed to the ionic nature of the  $\text{Li}^+$  ions between the  $\text{V}_3\text{O}_8$  layers and the smaller value of  $N(E_F)$  at the Li nucleus. The progressive shift of the Li resonances in the 4.2–3.0 V range is consistent with solid solution behavior in this region,<sup>11</sup>  $N(E_F)$  at Li increasing slowly as more lithium is inserted within the structure. Small variations between the shifts of different sites are ascribed to the differences in chemical environments and thus chemical and Knight shifts of these sites. However, there is one other alternative explanation for the shifts observed in the high-voltage region: hyperfine shifts are not observed in some  $\text{V}^{4+}$  compounds such as  $\beta\text{-LiVOPO}_4$ ,<sup>22</sup> even though this compound contains localized  $d^1$  electrons. This appears to be related to the location of the unpaired  $d^1$  electron in an orbital (most likely a  $d_{xy}$  orbital) that is not optimized for Li–O–V overlap, or possibly a combination of two opposing mechanisms. On the basis of the  $^7\text{Li}$  data only, it is difficult to rule out this latter possibility.

In contrast to the low potential region,  $^{51}\text{V}$  signals are detected for samples discharged to 3 V and above, the sample with average vanadium oxidation state of 4.83 ( $\text{Li}_{1.5}\text{V}_3\text{O}_8$ ) showing the highest resolution and most

intensity.  $^{51}\text{V}$  resonances for the  $\text{V}^{5+}$  ions in mixed  $\text{V}^{5+}/\text{V}^{4+}$  compounds may sometimes be "visible". For example, Delmaire et al.<sup>31</sup> assigned the resonance at  $-1447$  ppm observed in reduced forms of  $\text{Bi}_4\text{V}_2\text{O}_{11-\delta}$  to  $\text{V}^{5+}$  ions nearby  $\text{V}^{4+}$ ,  $d^1$  ions, the large shifts resulting from V–O– $\text{V}^{4+}$  hyperfine interactions between the  $\text{V}^{\text{V}}$  ions and the unpaired electrons located on  $\text{V}^{\text{IV}}$ . The connection between the vanadium polyhedra in  $\text{Li}_{1+x}\text{V}_3\text{O}_8$  is quite different from that in  $\text{Bi}_4\text{V}_2\text{O}_{10.66}$ :  $\text{V}^{\text{IV}}\text{O}_6$  octahedra share equatorial corners with two  $\text{V}^{\text{VO}}_4$  tetrahedra in the  $\text{Bi}_4\text{V}_2\text{O}_{10.66}$ <sup>32</sup> structure while the  $\text{VO}_6$  octahedra are edge-sharing in  $\text{Li}_{1+x}\text{V}_3\text{O}_8$ . Thus, the  $^{51}\text{V}$  MAS NMR hyperfine shift for  $\text{V}^{\text{V}}$  interacting with  $\text{V}^{\text{IV}}$  in the first or second coordination sphere in  $\text{Li}_{1+x}\text{V}_3\text{O}_8$  is not necessarily expected to be similar to that seen in  $\text{Bi}_4\text{V}_2\text{O}_{11-\delta}$ . Nonetheless, it is perhaps surprising that no shifted  $\text{V}^{5+}$  resonances are observed in the  $^{51}\text{V}$  MAS NMR spectra of  $\text{Li}_{1+x}\text{V}_3\text{O}_8$  and that partial reduction of vanadium does not result in a loss of signal intensity.

The  $^{51}\text{V}$  shift of the resonances, with increased intercalation level could, in principle, be ascribed to a chemical shift, a Knight shift, or a hopping process of the electrons between the  $\text{V}^{4+}$  and  $\text{V}^{5+}$  ions, the latter two mechanisms involving delocalization of the electrons on some or all of the vanadium sites in the  $\text{V}_3\text{O}_8$  layers. Very large shifts and short  $T_1$ 's are expected from a hopping mechanism, electron hopping resulting in considerable unpaired electron spin density at the V-nuclei for the atoms involved in the hopping process. If hopping involved all three sites, then all vanadium sites will be invisible to NMR. If the hopping involves only one site, then it may be possible to detect the other two sites. However, this mechanism does not explain the increase in signal at higher levels of intercalation. Furthermore, this mechanism will be strongly temperature-dependent, which is not consistent with our preliminary measurements of the pristine material.

$^{51}\text{V}$  spectra can be detected for metallic  $\text{V}^{4+}$  samples,<sup>33</sup> and large shifts may be observed as a result of the Knight shift, which is a measure of the Pauli paramagnetism (and thus the density of states  $N(E_F)$  at the vanadium nucleus). Several vanadium oxides, for example,  $\text{VO}$ ,  $\text{V}_2\text{O}_3$ , and  $\text{VO}_2$ , exhibit a phase transition from a low-temperature nonmetallic phase (semiconductor) to a metallic phase at higher temperatures.<sup>34–36</sup> Previous analysis of  $^{51}\text{V}$  MAS NMR spectra for the  $\beta$ -to  $\alpha\text{-VO}_2$  phase transition is accompanied by a large change in the shift from 2115 ppm to  $-4788$  ppm, a reduction in shift anisotropy and in signal intensity, reflecting the change from a nonmetallic to a metallic phase. The large shift at  $-4788$  ppm is ascribed to the Knight shift<sup>37</sup> and is consistent with the surprisingly large value of the Pauli paramagnetism of this material. Positive Knight shifts are expected when the conduction

(31) Delmaire, F.; Rigole, M.; Zhilinskaya, E. A.; Aboukais, A.; Hubaut, R.; Mairesse, G. *Phys. Chem. Chem. Phys.* **2000**, *2*, 4477.

(32) Joubert, O.; Jouanneaux, A.; Ganne, M. *Mater. Res. Bull.* **1994**, *29*, 175.

(33) Umeda, J. I.; Kusumoto, H.; Narita, K. *J. Phys. Soc. Jpn.* **1966**, *21*, 619.

(34) Morin, F. J. *Phys. Rev. Lett.* **1959**, *3*, 34.

(35) Cox, P. A. In *Solid State Chemistry Compounds*; Cheetham, A. K., Day, P., Eds.; Clarendon Press: Oxford, 1992; pp 1–30.

(36) Skibsted, J.; Nielsen, N. Chr.; Bildsoe, H.; Jakobsen, H. J. *Chem. Phys. Lett.* **1992**, *188* (5–6), 405.

(37) Nielsen, U. G.; Skibsted, J.; Jakobsen, H. J. *Chem. Phys. Lett.* **2002**, *356*, 73.

(28) Gaubicher, J. Unpublished results.

(29) Schumacher, R. T.; VanderVen, N. S. *Phys. Rev.* **1966**, *144*–1, 357.

(30) Nakagawa, Y.; Wang, S.; Matsumura, Y.; Yamaguchi, C. *Synth. Met.* **1997**, *85*, 1363.



process primarily involves  $s$  electrons, as is the case for, for example, Li metal. Conduction processes involving  $d$  electrons do not directly result in large values of  $N(E_F)$  at the vanadium nuclei. Instead, the Knight shifts arise from an indirect mechanism that involves a polarization of the core ( $s$ ) electrons, and negative shifts can be observed (e.g., for  $\text{VO}_2$ ). A much smaller Knight shift is seen for  $\text{V}_2\text{O}_3$ , which is closer to the shifts seen in this study: a broad resonance at  $-380$  ppm was observed in the wide-line NMR spectrum of this compound<sup>27</sup> and the MAS spectrum of this compound, obtained as part of this study, shows a resonance at  $-475$  ppm. A second, metastable phase of  $\text{VO}_2$  also shows metallic behavior at room temperature, but NMR spectra of this material have not been obtained, to date.

The dramatic loss of the  $^{51}\text{V}$  signal and broadening of the peaks for the 2.8 V sample spectrum appears to be consistent with an electronic transition from a system with delocalized electrons to an insulator with unpaired electrons localized on the vanadium centers. Some signal remains, however, and the shift of the most apparent observed isotropic resonance of this sample ( $-540$  ppm) is consistent with the progressive shift to higher frequencies seen on reduction from 4.2 to 3.0 V, suggesting that some of the electrons are still delocalized or, more likely, that the system is not fully in equilibrium.

Note that a small  $^7\text{Li}$  resonance at approximately  $-10$  ppm is observed in the 4.02 V sample (an even weaker resonance is observed in the 3.4 V sample at  $-15$  ppm). These resonances are tentatively ascribed to localized  $\text{V}^{4+}$  ions present as defects. This is consistent with the poorer  $^{51}\text{V}$  resolution of the 4.02 V sample. In conclusion, the electronic properties for the high- and low-voltage regions are quite distinct, in agreement with the phase transition seen by CV that separates these two regions. The low-voltage region comprises a mixed  $\text{V}^{4+}/\text{V}^{5+}$  semiconducting phase (from 2.8 to 2.7 V) and fully reduced  $\text{V}^{4+}$  phase at 2.5 V. The electronic properties of the high-voltage region do not result in large Li or V hyperfine shifts, possibly suggesting some metallic behavior or localization of electrons in orbitals that are not optimized for Li–O–V overlap. Further experiments, including ESR and magnetic susceptibility measurements, are now in progress to distinguish between these two possibilities.

### Conclusions

$^{51}\text{V}$  and  $^7\text{Li}$  MAS NMR combined with XRD and electrochemical cycling have been used to follow the

lithium intercalation process and study the corresponding mechanism. At high potentials, the  $^{51}\text{V}$  and  $^7\text{Li}$  resonances of  $\text{Li}_{1+x}\text{V}_3\text{O}_8$  shift gradually with Li intercalation level. This behavior is consistent with the single-phase behavior in the 4.2–3.0 V ( $0 < x < 1$ ) range. The  $^{51}\text{V}$  spectra in this region cannot be explained using a simple structural model that contains only three vanadium local environments: five  $^{51}\text{V}$  NMR resonances can be resolved at high spinning speeds, which are ascribed to both the three different crystallographic sites and to differences in the number of Li ions in the nearby cation coordination shell. The  $^7\text{Li}$  NMR spectra in this region contain a number of resonances, which are ascribed to Li ions in the octahedral and tetrahedral sites between the  $\text{V}_3\text{O}_8$  layers. Even for  $\text{LiV}_3\text{O}_8$ , both octahedral and tetrahedral sites are occupied, in contradiction to the diffraction studies of this material.<sup>9,11</sup> The  $^7\text{Li}$  NMR spectra are consistent with the filling of different lithium sites (e.g., Li5 and Li6), and rearrangement of Li ions between the sites, during the intercalation process. Since several  $T_d$  sites are filled in the composition range between  $\text{Li}_1\text{V}_3\text{O}_8$  and  $\text{Li}_{1.5}\text{V}_3\text{O}_8$ , the spectra are more readily rationalized based on the model of Jouanneau et al.,<sup>10,12</sup> rather than the model proposed by Benedek<sup>13</sup> where the lithium is inserted in only one  $T_d$  site for composition up to 1.5 lithium ions per unit formula.

For  $x > 1$ , new  $^7\text{Li}$  resonances with much larger negative (hyperfine) shifts are observed due to Li ions nearby  $\text{V}^{4+}$ . The appearance of these resonances is correlated with the broadening and then disappearance of the  $^{51}\text{V}$  resonances. The size and direction of the hyperfine shifts are similar to those seen in other layered materials. This behavior is consistent with the localization of the unpaired  $d$  electrons on the vanadium ions of the  $\text{V}_3\text{O}_8$  layers and suggests that the electronic phase transition, which occurs from 3.0 to 2.8 V, based on earlier electrochemical and X-ray diffraction studies,<sup>12</sup> may be due to charge ordering. The study highlights the complexity of these materials and the need to combine both long-range and short-range probes of structure to examine the intercalation mechanisms in these materials.

**Acknowledgment.** C.P.G. thanks the NSF (Grant DMR0211353) and the Camille and Henry Dreyfus Foundation (via a Teacher-Scholar Award) for support. CM034845W